Asia-Pac. J. Atmos. Sci., 52(2), 129-137, 2016 pISSN 1976-7633 / eISSN 1976-7951
DOI:10.1007/s13143-016-0014-z

Time of Emergence of Anthropogenic Warming Signals in the Northeast Asia Assessed from Multi-Regional Climate Models

Donghyun Lee[1], Seung-Ki Min[1], Changyong Park[1], Myoung-Seok Suh[2], Joong-Bae Ahn[3], Dong-Hyun Cha[4], Dong-Kyou Lee[5], Song-You Hong[6], Seong-Chan Park[7], and Hyun-Suk Kang[8]

[1]*School of Environmental Science and Engineering, Pohang University of Science and Technology, Pohang, Korea*
[2]*Department of Atmospheric Science, Kongju National University, Kongju, Korea*
[3]*Department of Atmospheric Sciences, Pusan National University, Busan, Korea*
[4]*School of Urban and Environmental Engineering, Ulsan National Institute of Science and Technology, Ulsan, Korea*
[5]*School of Earth and Environmental Sciences, Seoul National University, Seoul, Korea*
[6]*Korea Institute of Atmospheric Prediction Systems, Seoul, Korea*
[7]*Korea Meteorological Administration, Seoul, Korea*
[8]*National Institute of Meteorological Sciences, Jeju, Korea*

(Manuscript received 1 November 2015; accepted 30 March 2016)

Abstract: Time of Emergence (ToE) is the time at which the signal of climate change emerges from the background noise of natural climate variability, and can provide useful information for climate change impacts and adaptations. This study examines future ToEs for daily maximum and minimum temperatures over the Northeast Asia using five Regional Climate Models (RCMs) simulations driven by single Global Climate Model (GCM) under two Representative Concentration Pathways (RCP) emission scenarios. Noise is defined based on the interannual variability during the present-day period (1981-2010) and warming signals in the future years (2021-2100) are compared against the noise in order to identify ToEs. Results show that ToEs of annual mean temperatures occur between 2030s and 2040s in RCMs, which essentially follow those of the driving GCM. This represents the dominant influence of GCM boundary forcing on RCM results in this region. ToEs of seasonal temperatures exhibit larger ranges from 2030s to 2090s. The seasonality of ToE is found to be determined majorly by noise amplitudes. The earliest ToE appears in autumn when the noise is smallest while the latest ToE occurs in winter when the noise is largest. The RCP4.5 scenario exhibits later emergence years than the RCP8.5 scenario by 5-35 years. The significant delay in ToEs by taking the lower emission scenario provides an important implication for climate change mitigation. Daily minimum temperatures tend to have earlier emergence than daily maximum temperature but with low confidence. It is also found that noise thresholds can strongly affect ToE years, i.e. larger noise threshold induces later emergence, indicating the importance of noise estimation in the ToE assessment.

Key words: Time of emergence, regional climate models, RCP scenarios, Northeast Asia

1. Introduction

The observed global and continental-scale warming since the mid-20th century has been attributed to human influences with high confidence (Bindoff et al., 2013). However, causes of the observed climate changes on regional and local scales remain quite uncertain due partly to the increased influences of natural variability (e.g., Deser et al., 2012). Reliable projections of future climate changes and corresponding impact assessments are required on smaller spatial scales. Particularly, localized information on changes in weather and climate extremes is importantly needed to evaluate and select adaptation strategies (Seneviratne et al., 2012).

There are three key sources inducing uncertainty in future climate change: external forcing, model response, and internal variability (Tebaldi and Knutti, 2007; Hawkins and Sutton, 2009). Forcing-driven uncertainty is associated with insufficient information of external factors such as future anthropogenic emissions of greenhouse gases (GHG) and aerosols and land use change. Different models produce different responses to the same forcing due to structural uncertainties in physical and dynamical configurations of the climate system. The last source, internal variability is the natural variability of the coupled climate system arising mainly from interaction between atmosphere and ocean without influence of external forcing (Deser et al., 2012).

A well-known approach to assessing these uncertainty factors is to search for the time when the signal of climate change exceeds its natural variability, so-called Time of Emergence (ToE; Hawkins and Sutton, 2012). The ToE and similar methods have been increasingly developed and applied to global and regional studies (Christensen et al., 2007; Giorgi and Bi, 2009; Hawkins and Sutton, 2009, 2012; Maraun, 2013; Sui et al., 2014; King et al., 2015, 2016). Based on datasets of multiple global climate model (GCM) simulations available from the Coupled Model Intercomparison Project Phase 3 (CMIP3) and Phase 5 (CMIP5), previous studies consistently reported that the signals of anthropogenic climate changes would emerge against the natural climate variability for global and regional temperatures and precipitation (Giorgi and Bi.,

Corresponding Author: Seung-Ki Min, School of Environmental Science and Engineering, Pohang University of Science and Technology, Pohang 37673, Korea.
E-mail: skmin@postech.ac.kr

2009; Hawkins and Sutton, 2009, 2012) and their extremes (King et al., 2015).

East Asia is expected to experience continued warming and moistening in the 21st century future (e.g., Christensen et al., 2007, 2013 and references therein; Yun et al., 2012; Baek et al., 2013), consistent with the observed increases in frequency and intensity of hot extremes (e.g., Min et al., 2014, 2015). To address the demand for adaptation measures on much smaller spatial scales than those simulated by GCM, there have been increasing efforts to produce fine-scale climate information using regional climate models (RCMs) over East Asia region (Christensen et al., 2007, 2013; Im et al., 2008, 2012a, 2012b; Hong and Chang, 2012; Suh et al., 2012; Oh et al., 2013; Lee and Hong, 2014; Hong and Kanamitsu, 2014; Park et al., 2016). However, studies on ToE for East Asia have been very limited (Sui et al., 2014), particularly based on RCM outputs.

In this study, we apply a ToE approach to high-resolution multiple RCM simulations over the Northeast Asia focusing on emergence timing of the warming signals. Further, the influence of external anthropogenic forcing is examined by comparing two RCP scenarios (RCP4.5 and RCP8.5), which would be useful for climate change mitigation and adaptation. We also investigate locations and seasons with earlier ToEs by examining signal and noise patterns. In Section 2 the data and methods used are described. In Section 3 ToE estimates are analyzed with some comparisons and sensitivity tests. Summary and discussions are given in Section 4.

2. Data and methods

We use Climatic Research Unit Time Series (CRU TS) data (Harris et al., 2014, version 3.22) as observations for surface air temperature, which are station-based monthly dataset with high resolution of 0.5^o longitude × 0.5^o latitude. Monthly mean daily maximum and minimum temperatures (hereinafter referred to as Tmax and Tmin, respectively) are used for the Northeast Asian domain defined as 30^{o}N-44^{o}N and 117^{o}E-138^{o}E.

Five RCMs (HadGEM3-RA, RegCM4, SNU-RCM, WRF, and GRIMs) analyzed in this study are listed in Table 1 with model configurations including dynamics and physics such as cloud physics and land surface schemes [refer to Suh et al., (2016) for more details]. These five RCMs were driven by an identical boundary condition obtained from the HadGEM2-AO GCM (Baek et al., 2013). Single member experiment has been performed for each RCM for historical period (1981-2010, with natural plus anthropogenic forcing) and future period (2021-2100, for two RCP scenarios). The RCP scenarios are new emission scenarios developed for the 5th Assessment Report of the Intergovernmental Panel on Climate Change (IPCC) to take into account future changes in radiative forcing as well as the way of human society's responses through changes in technology, economies, and policy (Moss et al., 2010). There are the four available RCP scenarios and this study considers the RCP4.5 and RCP8.5 scenarios. The RCP4.5 is a relatively optimistic scenario in which GHG emissions peak around 2040 and then decline, resulting in a radiative forcing of 4.5 W m^{-2} at stabilization after 2100. In contrast, the RCP8.5 is a 'rising' pathway scenario where GHG increases throughout the 21st century with a radiative forcing reaching about 8.5 W m^{-2} in 2100. Prior to analysis, all RCM data (12.5 km × 12.5 km resolution) are interpolated onto the same grids of 0.5^o longitude × 0.5^o latitude. To obtain overall RCM results, we construct MME (multi-model ensemble) means, which are simply arithmetic averages of the results from all five RCMs. In order to assess the influence of GCM boundary forcing, HadGEM2-AO results are also used on its original horizontal resolution of 1.875^o longitude × 1.25^o latitude.

Noise and signal can be defined differently depending on the question. Since our study focuses on identification of ToE in the near future climate relative to a current condition, we use present 30 years (1981-2010) as a base period and estimate signal and noise accordingly. First, temperature anomalies during the whole analysis period (1981-2100) are calculated relative to each 1981-2010 mean. Future temperature anomalies themselves become signal (S) representing temperature responses to a given RCP scenario forcing at each grid point for each RCM. Second, interannual standard deviation (σ) of temperatures is obtained from the current 30 year period and the noise (N) is defined as doubled standard deviation (2σ). This noise estimate is equivalent to taking about 97.5th

Table 1. List of five RCMs used in this study.

	HadGEM3-RA	RegCM4	WRF	SNU-RCM	GRIMs
# of grid points	180 × 200	180 × 200	180 × 201	180 × 200	182 × 201
Vertical level	Hybrid-38	σ-23	Eta-28	σ-24	σ-28
Dynamic Framework	Non-hydrostatic	Hydrostatic	Non-hydrostatic	Non-hydrostatic	Hydrostatic
Microphysics scheme	Single moment bulk scheme	SUBEX	WSM3	Reisner2	WSM1
PBL scheme	Nonlocal scheme	Holtslag	YSU	YSU	YSU+stable BL
Convection scheme	Revised mass flux scheme	MIT-Emanuel	Karin-Fritsch II	Karin-Fritsch II	SAS+CMT
Land surface	MOSES-II	CLM3.5	Noah	CLM3.0	OML-climatology value
Radiation scheme	Generalized 2-stream	CCM3	CAM	CCM2	GSFC
Spectral nudging	No	Yes	No	Yes	Yes

percentile of temperature anomalies from the present climate period, assuming normal distributions. We employ this strict threshold to consider that a 30-year period could be rather short to represent a full range of natural internal variations.

Finally, given signal and noise estimates, the ToE is defined as the first year when the magnitude of the signal becomes greater than noise, i.e. signal-to-noise ratio (S/N) is larger than one (S/N > 1) with permanent emergence after ToE year (practically until 2100). We limit ToE estimation until 2090 to allow minimum 10 years for permanent emergence. However, when testing significance of ToE differences (see below), we use ToE obtained for 2091-2100 assuming that temperatures will keep rising beyond 2100. To explore the importance of noise thresholds, we test sensitivity of our ToE estimates to different noise thresholds of 1σ and 3σ.

In order to test significance of differences in ToE estimates from five RCM pairs, which cannot usually be assumed to be normally distributed, we use the Wilcoxon signed-rank test (Wilcoxon, 1945) that is a non-parametric hypothesis test used when comparing two paired samples. Especially, we examine whether there is a significant difference in ToEs between two RCP scenarios and between Tmax and Tmin.

3. Results

a. Annual temperatures

ToEs of annual mean temperatures are first analyzed. Figure 1 displays time series of annual mean Tmax and Tmin averaged over the Northeast Asian land. Note the unit of S/N calculated from five individual RCMs and GCM for two RCP scenarios. It can be seen that temporal variations in Tmax and Tmin of RCMs essentially follow those of the driving GCM during the entire period (1981-2100), including long-term trends and year-to-year fluctuations. This represents the dominant influence of GCM boundary forcing on downscaled results in this region. ToEs of RCMs and GCM are displayed as vertical lines (Fig. 1). Warming signals beyond natural variability noises emerge from 2035 under both RCP scenarios. A slower emergence appears around year 2047 for Tmax in the RCP4.5 scenario. There is a good agreement in ToEs among RCMs, again indicating the strong influence of identical GCM forcing (e.g., Christensen et al., 2013; Park et al., 2016; Suh et al., 2016). The one exception is that HadGEM3-RA exhibits a bit later ToEs than other RCMs, which is due to relatively smaller warming signal and larger noise (not shown). The smaller warming of HadGEM3-RA during the mid-21st century is consistent with the result of Suh et al. (2016).

ToEs of RCMs are well consistent with those of GCMs in spite of different horizontal resolutions. The GCM signal is slightly stronger than those of RCMs (Suh et al., 2016). However, noise is also slightly greater in GCM (Tmax: 1.56 K; Tmin: 1.25 K) than RCMs (Tmax: 1.24 K; Tmin: 1.17 K). GCM's stronger amplitude in both signal and noise makes its ToE (and S/N) similar to those of RCMs.

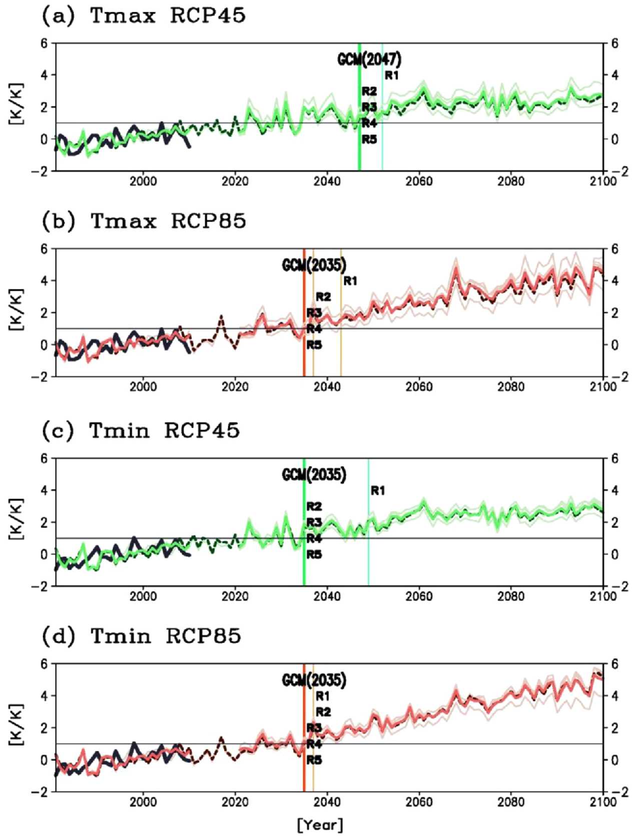

Fig. 1. Time series of signal-to-noise ratio (S/N) [K/K] for annual mean Tmax and Tmin anomalies averaged over the Northeast Asia land area for the RCP 4.5 and 8.5 scenarios, and Time of Emergence (ToEs, vertical lines with values for GCM). Colored solid lines indicate RCM results (light: each RCM, dark: RCM-MME). Black solid lines are observations and black dashed-lines are GCM results. R1 to R5 represents five RCMs as listed in the Table 1. Black horizontal line indicates S/N = 1 and all values lie above this line after ToE (S/N > 1). See text for details of the definition of signal (S) and noise (N).

In order to further understand differences in signal and noise between GCM and RCMs, we compare spatial distributions of ToE, signal strength on the mid-21st century (measured as 2041-2070 means of temperature anomalies), and noise strength. The results for Tmax under the RCP8.5 scenario (Fig. 2) show that ToE years generally come earlier over the ocean area (mean ToE: 2036) than in the land area (mean ToE: 2039) in RCMs. Overall spatial patterns of signal and noise strengths are similar between GCM and RCM-MME, characterized by larger signal and larger noise in the land area than in the ocean. A good agreement between GCM and RCMs is seen over the ocean area for both signal (GCM: 2.45 K; RCM-MME: 2.48 K) and noise strength (GCM: 1.17 K; RCM-MME: 0.97 K). However, considerable GCM-RCM differences occur in land areas. Particularly, in the Korean peninsula and the central-eastern and northeastern China, RCMs display much weaker signals than GCM, contributing to later ToE over the land area than GCM. GCM-RCM difference in ToE is also noticeable

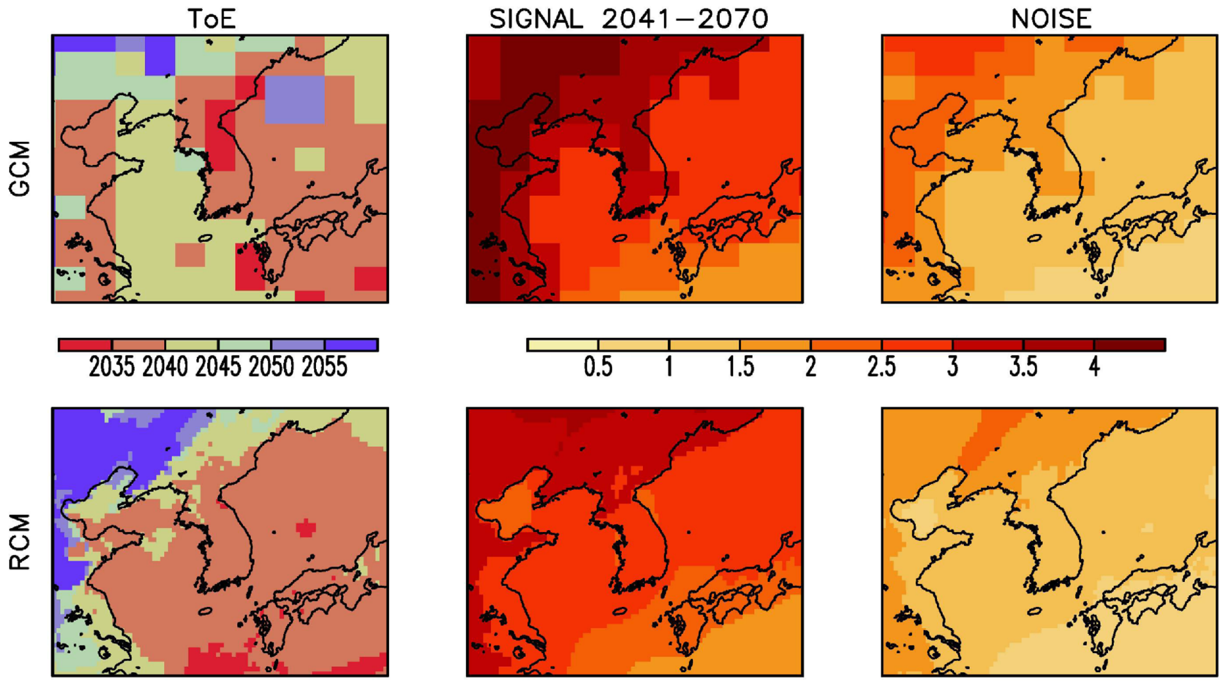

Fig. 2. Time of Emergence [year], signal [K], and noise [K] for annual mean Tmax under the RCP8.5 scenario obtained from GCM (upper) and RCM-MME (lower). Here signals represent mean temperature anomalies over the mid-21 century (2041-2070) relative to the present day climatology (1981-2010).

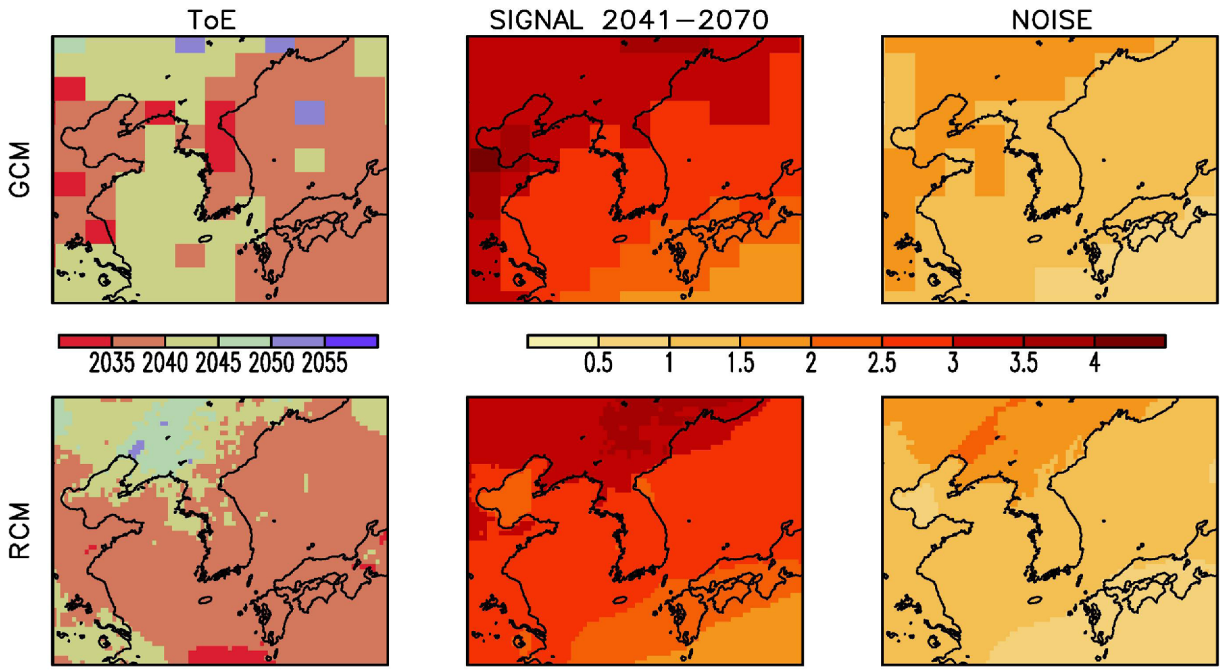

Fig. 3. Same as Fig. 2 except for annual mean Tmin.

over the Yellow Sea, which seems to be related to the stronger signal over the eastern China in GCM. The cause of the GCM-RCM differences over land is uncertain, but the stronger difference in summer (Suh et al., 2016) suggests that this discrepancy might be related to different responses in cloud cover between GCM and RCMs (also see below our discussion on the Tmax and Tmin comparison). Note that large inter-RCM differences in ToEs exist in the northeastern China

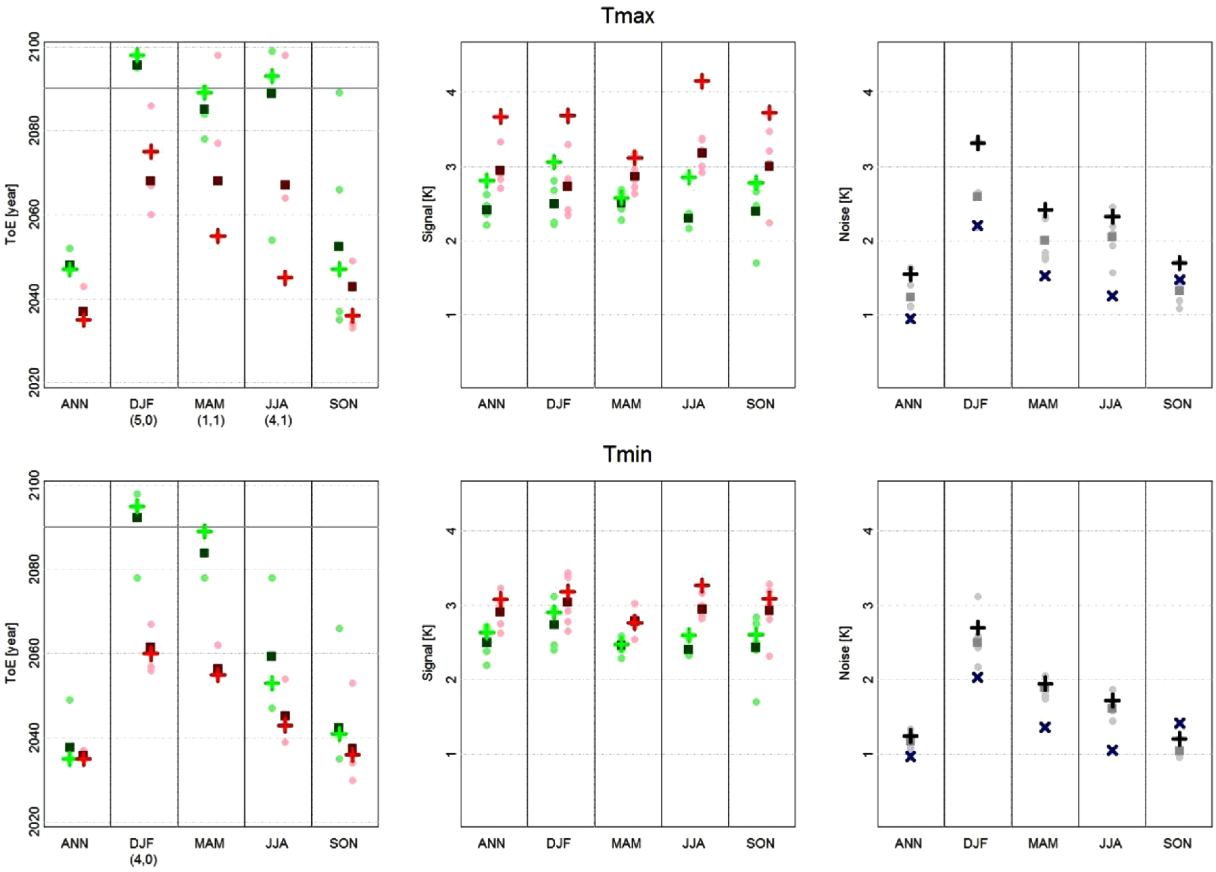

Fig. 4. Distribution of ToE [year], signal [K], and noise [K] for Tmax (upper) and Tmin (lower) averaged over the Northeast Asia land area. Each plot shows results for annual (ANN), DJF, MAM, JJA, and SON means. Cross indicates GCM, circle represents each RCM, and squares are RCM-MME results. Noise estimate from observations is shown by blue × mark. Two colors represent the RCP4.5 (green) and RCP 8.5 (red) scenarios. ToEs obtained for 2091-2100 are included assuming that temperatures will keep rising beyond 2100. Two numbers in parentheses in the horizontal axis of ToE results indicate number of RCMs having ToEs during 2091-2100 for the RCP 4.5 (first) and RCP 8.5 scenarios (second number).

(e.g., RCM-MME: 2060s; HadGEM3-RA: 2070s; SNU-RCM: no ToE), which represent different RCM responses probably due to different model configurations (Table 1).

Spatial patterns of ToE for Tmin resemble those for Tmax (Fig. 3). However, there are notable differences. Tmin has slightly weaker warming signal than Tmax over land, which is seen more clearly in GCM. In this respect, previous studies rather projected stronger warming in Tmin than in Tmax as a results of effects of increases in cloud cover and aerosols that reduce daytime solar heating (e.g. Zhou et al., 2009 and references therein). Thus, this smaller increasing trend in Tmin is likely to be related to cloud and aerosol characteristics of HadGEM2-AO, which needs further investigation. Figure 3 also shows that noise over land is weaker in Tmin than in Tmax, representing smaller inter-annual variability in nighttime than daytime temperatures. Causes of this feature also remain unclear. As a result, smaller amplitudes in both signal and noise for Tmin make S/N and ToE patterns similar to those for Tmax.

b. Seasonal temperatures

It would be useful to know which season(s) will have earlier emergence of warming signals than other seasons and also to understand what makes the seasonal difference. In this respect, we compare seasonal ToEs averaged over the Northeast Asia land area where temperature seasonality is relatively large. Also since RCMs are driven by the identical ocean boundary condition, we focus on land in order to compare effects of atmospheric dynamic downscaling. Figure 4 shows ToE, signal, and noise for Tmax (upper) and Tmin (lower panel) for boreal winter (December-Feburary, DJF), spring (March-May, MAM), summer (June-August, JJA), and autumn (September-November, SON) seasons in comparison with annual mean results (ANN). ToEs between the RCP4.5 (green) and RCP8.5 (red) scenarios are compared. GCM results (cross mark) are also displayed.

Among four seasons, the earliest ToEs occur in autumn and the latest ToEs in winter. This ToE seasonality over the Northeast Asia is well consistent with the findings of Sui et al.

(2014) who used CMIP5 multiple GCM ensembles. Comparing ToEs with signal and noise amplitudes in terms of seasonality reveals that noise of the internal natural variability is a dominant factor determining seasonal ToEs. Smaller natural variability in autumn explains the earlier ToE and larger natural variability in winter leads to the later ToE than other seasons. It seems that the seasonal pattern of noise represents seasonality of climate variability affecting the North Asia. For example, the Arctic Oscillation is known to affect Korea and East Asia during winter and spring more strongly than other seasons, and stronger influence of El-Niño Southern Oscillation appears during winter as reviewed by Min et al. (2015). Summer temperature in this region seems to have larger variability than autumn, due to possible influences of the East Asian summer monsoon and the intra-seasonal variability (Min et al., 2015). Further analysis is needed for a clear isolation of physical mechanisms for the seasonality of noise amplitude.

Modeled noise is overall larger than the observed noise (Fig. 4) as can also be seen in Fig. 1. This implies that RCMs do not underestimate the observed variability. Annual results exhibit earlier ToEs than seasonal results. This is consistent with relatively weaker noises in annual mean temperatures with variations being smoother by taking annual averages (Christensen et al., 2007; Sui et al., 2014).

There is not much difference in signal amplitudes across seasons, becoming a minor factor affecting the seasonality of ToEs over this region (Fig. 4). One example of signal impact on ToE can be seen from GCM results. Noise estimates are very similar between spring and summer in GCM. However, GCM predictions under the RCP8.5 scenario indicate larger warming (signal) in summer than spring, and this induces earlier ToE in summer than in spring. Another and more important example for the role of signal amplitude in determining ToEs is the earlier ToEs in the RCP8.5 scenario than in the RCP4.5 scenario. Warming signals are generally larger in the RCP8.5 scenario that has stronger anthropogenic forcing with higher greenhouse gas emissions as described above (Moss et al., 2010). We carry out a statistical test for this comparison (see below).

Although identical GCM boundary condition is applied to RCM simulations, Fig. 4 shows that seasonal ToE estimates from five RCMs can be highly uncertain, unlike annual results that show good inter-RCM agreement. The inter-RCM uncertainty in ToEs is again affected by inter-RCM spreads in both signal and noise, either of which varies much across seasons and scenarios. The origin of uncertainty sources may include RCM differences in physics. Given diverse physical schemes implemented across RCMs (Table 1), it is difficult to identify dominant factors explaining RCM differences, which is beyond the scope of this study. For example, Giorgi et al. (2012) systematically evaluated RCM dependency of physics schemes and their parameterizations for Europe. Further investigation for East Asia is warranted for this issue, with the help of relevant sensitivity experiments considering different physics schemes like land surface or convective parameterization (e.g., Kang and Hong, 2008; Li et al., 2015).

Table 2. Median value of differences in ToEs and signals (2041-2070 mean anomalies) between the RCP4.5 and RCP8.5 scenarios (RCP4.5 - RCP8.5) for Tmax and Tmin. Asterisk (*) and double asterisks (**) indicate 10% and 5% significance level, respectively, based on the Wilcoxon signed-rank test. See text for details.

ToE	Tmax [year]	Tmin [year]
ANN	+12**	0
DJF	+28**	+31**
MAM	+23*	+29**
JJA	+35**	+8*
SON	+2	+5**
Signal (2041-2070)	Tmax [K]	Tmin [K]
ANN	−0.45**	−0.36**
DJF	−0.09**	−0.11**
MAM	−0.17**	−0.18**
JJA	−0.42**	−0.33**
SON	−0.46**	−0.46**

c. Scenario differences

As discussed above, in terms of scenario difference, intensified warming occurs under the RCP8.5 scenario for both Tmax and Tmin, which leads to earlier ToE than under the RCP4.5 scenario. We conduct the Wilcoxon signed-rank test to check whether these differences are statistically significant between two RCP scenarios. Table 2 shows results for median differences in ToEs and signals between two scenarios (RCP4.5 value - RCP8.5 value) with significant levels for annual mean and four seasons. For ToE differences, except for two cases (annual Tmin and autumn Tmax), all cases exhibit statistically significant differences between two RCP scenarios (6 cases significant at 5% significance level and 2 cases at 10% level). Reduced emissions in the RCP4.5 scenario is found to delay ToEs by 12 years for annual Tmax with ranging from 5 to 35 years depending on seasons and variables.

Differences in signal amplitudes are tested in the same way (Table 2) for the mid-21st century (2041-2070) when many ToEs are observed. Significant differences are found in all seasons and for both Tmax and Tmin at 5% significance level. About 0.1 K to 0.5 K warming is reduced in the mid-21st century by taking less emission scenarios. This clearly shows that different emission (or mitigation) scenario will deliver different radiative forcing, which in turn will induce different warming signals and affect ToE.

Scenario difference affects both Tmax and Tmin, but which one will show earlier emergence between daytime and night-time temperatures would be a useful question, considering impact on hot extremes (Seneviratne et al., 2012; Donat and Alexander, 2012; Min et al., 2014; King et al., 2015). To

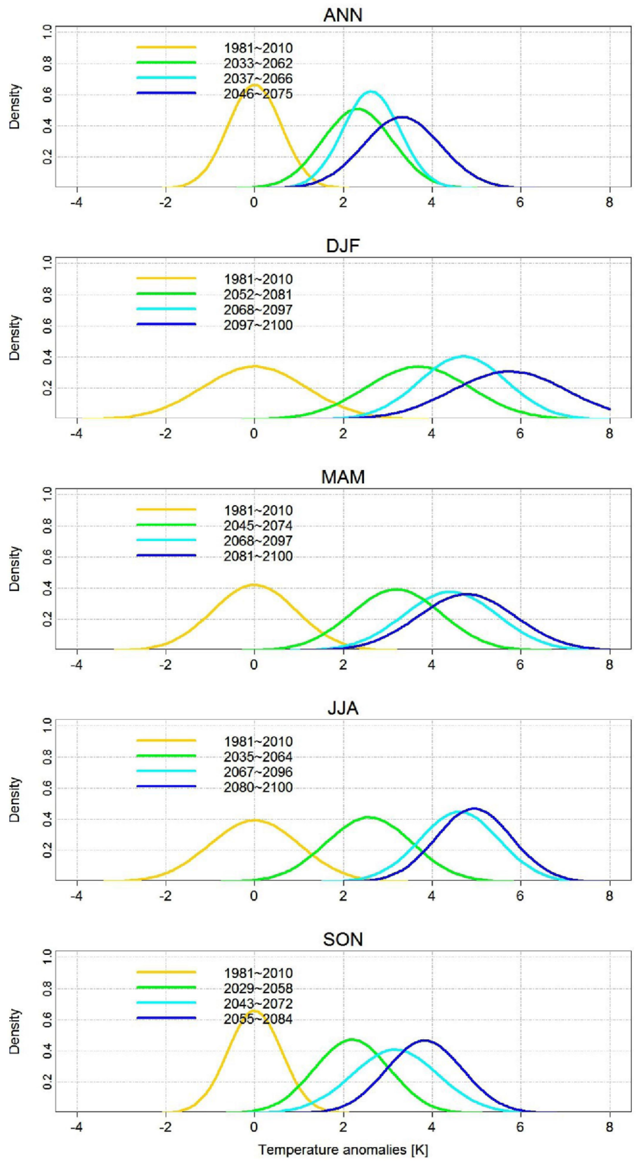

Fig. 5. Fitted distribution of Tmax anomalies from RCM-MME for the present period (1981-2010; yellow) and future 30-year periods from the RCP8.5 scenario after ToE year when using different noise thresholds of 1σ (green), 2σ (cyan), and 3σ (blue). ToEs for RCM-MME are obtained from taking multi-RCM averages of ToEs from individual RCMs, consistent with Fig. 4.

explore this point, ToEs and signals are compared between Tmax and Tmin following the way used for scenario differences (not shown). Results show that Tmin warming tends to be faster than Tmax on average, resulting in earlier emergence. However, differences in ToEs between Tmax and Tmin are not statistically significant in many cases. It should also be noted that this ToE difference between Tmax and Tmin can be a GCM-dependent result as discussed above.

d. Noise thresholds

Anthropogenic warming signals will emerge earlier when using lower threshold for signal-to-noise ratio (Hawkins and Sutton, 2012). However, different definition of noise may have non-linear impacts on some ToEs. Here we test sensitivity of ToEs to the use of different noise threshold by varying noise from one standard deviation (1σ) to three standard deviation (3σ). This corresponds to 50% decrease in noise (or doubled S/N) and 50% increase in noise (or reduced S/N by 67%), respectively, compared to the original noise definition (2σ). For better understanding, we compare distributions of temperature anomalies drawn for the current 30-year period and those for three future 30-year periods after ToE year, which are obtained from different noise thresholds. Figure 5 displays results for Tmax under the RCP8.5 scenario. Comparison of two distributions of noise and signal apparently shows from when the future climate signals are separated from ranges of the internal climate variability, depending on selected noise thresholds. As the stricter noise threshold is applied, the later ToEs are obtained with temperature anomaly distributions shifting to the right into warmer conditions.

It is notable that sometimes ToE shifts occur in a nonlinear fashion according to different noise thresholds. For instance, ToE of annual Tmax does not show a significant change when applying 1σ (2033) and 2σ (2037), respectively. Then a sudden shift of ToE to 2046 happens when 3σ is used, representing a nonlinear inherent nature of ToE. A similar nonlinear shift of ToE can be seen in DJF Tmax (Fig. 5). This also highlights the necessity of uncertainty assessments in ToE with considering possible ranges of noise and signal estimates based on larger model samples, particularly for small scale analyses (Mahlstein et al., 2011; Hawkins and Sutton, 2012; Sui et al., 2014).

4. Summary and discussion

This study evaluates Time of Emergence (ToE) of daily maximum and minimum temperatures (Tmax and Tmin) using five RCMs simulated under the RCP4.5 and RCP8.5 scenarios forced by single GCM. Noise of the natural climate variability is estimated from the present period (1981-2010) and then emergence timing of future warming signals beyond the noise level is obtained for each RCM and each scenario. Here we apply a strict noise threshold as two standard deviations (2σ) to consider possible underestimations of the internal variability due to a relatively short period. ToEs from five RCMs are compared with GCM results and also differences between scenarios and variables are examined to explore contribution factors determining ToEs. Main conclusions from our analyses are as follows.

- ToEs from multiple RCMs are very similar to those from the driving GCM that provided boundary conditions to RCMs, confirming the strong influence of GCM boundary forcing on RCM outputs for the Northeast Asia (Christensen et al., 2013; Park et al., 2016; Suh et al., 2016). However, different ToEs from GCM are seen over land areas where inter-RCM differences are also large, possibly due to different model configurations such as land surface and/or convection schemes.

· Results from seasonal ToE analyses show that autumn season has the earliest ToE while winter has the latest ToE, consistent with previous study (Sui et al., 2014). Noise is found to be a dominant factor affecting seasonal difference in ToEs with signal being a secondary one. Seasons with smaller noise tend to have earlier ToEs and seasons with larger noise exhibit later ToEs.
· Significantly different ToEs and signals are obtained between the RCP4.5 and RCP8.5 scenario results, indicating later ToEs under the RCP4.5 scenario by 5-35 years. This means that taking lower emission scenarios like the RCP4.5 would delay the emergence timing of anthropogenic warming signals. Tmin tends to have earlier emergence than Tmax but the difference is not robust.
· There is high sensitivity of ToEs to the use of different noise thresholds, indicating the importance of noise estimate. More strict (larger noise) threshold induces later ToE and vice versa. In some cases, the delay in emergence years shows nonlinearity, which might be due to anomalous cold years that inherently occur in the climate change signal (Deser et al., 2012).

Our study provides the first ToE analysis for East Asia based on multiple RCMs with a systematic investigation of signal and noise contribution to ToEs. However, our study has a caveat arising from the use of single driving GCM, which may transfer systematic biases of the GCM into downscaled RCM outputs, limiting full realization of inter-RCM uncertainties. For more reliable estimate of ToEs, it is required to assess uncertainty factors more comprehensively with taking account of inter-GCM differences.

Acknowledgements. This work was funded by the Korea Meteorological Administration Research and Development Program under Grant KMIPA 2015-2082.

Edited by: Sang-Woo Kim and Sang-Wook Yeh

References

Baek, H. J., and Coauthors, 2013: Climate change in the 21st century simulated by HadGEM2-AO under representative concentration pathways. *Asia-Pac. J. Atmos. Sci*., **49**, 603-618.

Bindoff, N. L., and Coauthors, 2013: Detection and attribution of climate change: From global to regional. In *Climate Change 2013: The Physical Science Basis. Contribution of Working Group I to the Fifth Assessment Report of the IPCC*. Cambridge University Press, 867-952.

Christensen, J. H., and Coauthors, 2007: Regional climate projections. In *Climate Change, 2007: The Physical Science Basis. Contribution of Working Group I to the Fourth Assessment Report of the IPCC*. Cambridge University Press, 847-940.

______, and Coauthors, 2013: Climate phenomena and their relevance for future regional climate change. In *Climate Change 2013: The Physical Science Basis. Contribution of Working Group I to the Fifth Assessment Report of the IPCC*, Cambridge University Press, 1217-1308.

Deser, C., A. Phillips, V. Bourdette, and H. Teng, 2012: Uncertainty in climate change projections: the role of internal variability. *Clim. Dynam*., **38**, 527-546.

Donat, G. M., and L. V. Alexander, 2012: The shifting probability distribution of global daytime and night-time temperatures. *Geophys. Res. Lett*., **39**, L14707, doi:10.1029/2012GL052459.

Giorgi, F., and X. Bi, 2009: Time of emergence (TOE) of GHG-forced precipitation change hot-spots: *Geophys. Res. Lett*., **36**, L06709, doi:10.1029/2009GL037593.

______, and Coauthors, 2012: RegCM4: model description and preliminary tests over multiple CORDEX domains. *Clim. Res*., **52**, 7-29.

Harris, I., P. D. Jones, T. J. Osborn, and D. H. Lister, 2014: Updated high-resolution grids of monthly climatic observations-the CRU TS3. 10 Dataset, *Int. J. Climatol.,* **34**, 623-642.

Hawkins, E., and R. Sutton, 2009: The potential to narrow uncertainty in regional climate predictions. *Bull. Amer. Meteor. Soc.*, **90**, 1095-1107.

______, and ______, 2012: Time of emergence of climate signals: *Geophys. Res. Lett*., **39**, L01702, doi:10.1029/2011GL050087.

Hong, S.-Y., and E.-C. Chang, 2012: Spectral Nudging Sensitivity Experiments in a Regional Climate Model. *Asia-Pac. J. Atmos. Sci.*, **48**, 345-355.

______, and M. Kanamitsu, 2014: Dynamical downscaling: Fundamental issues from an NWP point of view and recommendations. *Asia-Pac. J. Atmos. Sci.*, **50**, 83-104, doi:10.1007/s13143-014-0029-2.

Im, E.-S., J.-B. Ahn, W.-T. Kwon, and F. Giorgi, 2008: Multi-decadal scenario simulation over Korea using a one-way double-nested regional climate model system. Part 2: future climate projection (2021-2050). *Clim. Dynam*., **30**, 239-254.

______, B.-J. Lee, J.-H. Kwon, S.-R. In, and S.-O. Han, 2012a: Potential increase of flood hazards in Korea due to global warming from a high-resolution regional climate simulation. *Asia-Pac. J. Atmos. Sci.*, **48**, 107-113.

______, J.-B. Ahn, and D.-W. Kim, 2012b: An assessment of future dryness over Korea based on the ECHAM5-RegCM3 model chain under A1B emission scenario. *Asia-Pac. J. Atmos. Sci.*, **48**, 325-337.

Kang, H.-S., and S.-Y. Hong, 2008: Sensitivity of the simulated East Asian summer monsoon climatology to four convective parameterization schemes. *J. Geophys. Res.*, **113**, D15119 doi:10.1029/2007JD009692.

King, A. M., G. Donat, E. M. Fischer, E. Hawkins, L. V. Alexander, D. J. Karoly, A. J. Dittus, S. C. Lewis, and S. E. Perkins, 2015: The timing of anthropogenic emergence in simulated climate extremes. *Environ. Res. Lett*., **10**, 094015, doi:10.1088/1748-9326/10/9/094015.

______, M. T. Black, S.-K. Min, E. M. Fischer, D. M. Mitchell, L. J. Harrington, and S. E. Perkins-Kirkpatrick, 2016: Emergence of heat extremes attributable to anthropogenic influences. *Geophys. Res. Lett.*, published online, doi:10.1002/2015GL067448.

Lee, J.-W., and S.-Y. Hong, 2014: Potential for added value to downscaled climate extremes over Korea by increased resolution of a regional climate model. *Theor. Appl. Climatol.*, **117**, 667-677, doi:10.1007/s00704-013-1034-6.

Li, W., W. Guo, Y. Xue, C. Fu, and B. Qiu, 2015: Sensitivity of a regional climate model to land surface parameterization schemes for East Asian summer monsoon simulation. *Clim. Dynam*., doi:10.1007/s00382-015-2964-8.

Maraun, D., 2013: When will trends in European mean and heavy daily precipitation emerge? *Environ. Res. Lett.*, **8**, 014004, doi:10.1088/1748-9326/8/1/014004.

Mahlstein, I., R. Knutti, S. Solomon, and R. Portmann, 2011: Early onset of significant local warming in low latitude countries. *Environ. Res. Lett.*, **6**, 034009, doi:10.1088/1748-9326/6/3/034009.

Min, S.-K., Y. H. Kim, M. K. Kim, and C. Park, 2014: Assessing human contribution to the summer 2013 Korean heat wave, In: Explaining extreme events of 2013 from a climate perspective. *Bull. Amer. Meteor. Soc.*, **95**, S48-S51.

______, and Coauthors, 2015: Changes in weather and climate extremes over Korea and possible causes: A review. *Asia-Pac. J. Atmos. Sci.*, **51**, 103-121.

Moss, R., and Coauthors, 2010: The next generation of scenarios for climate change research and assessment. *Nature*, **463**, 747-756.

Oh, S. G., M. S. Suh, and D. H. Cha, 2013: Impact of lateral boundary conditions on precipitation and temperature extremes over South Korea in the CORDEX regional climate simulation using RegCM4. *Asia-Pac. J. Atmos. Sci.*, **49**, 497-509.

Park, C., and Coauthors, 2016: Evaluation of multiple regional climate models for summer climate extremes over East Asia. *Clim. Dynam*., **46**, 2469-2486, doi:10.1007/s00382-015-2713-z.

Seneviratne, S. I., and Coauthors, 2012: Changes in climate extremes and their impacts on the natural physical environment. In *Managing the Risks of Extreme Events and Disasters to Advance Climate Change Adaptation. A Special Report of Working Groups I and II of the IPCC*. Cambridge University Press, Cambridge, 109-230.

Suh, M.-S., S.-G. Oh, D.-K. Lee, D. H., Cha. S.-J. Choi, C.-S. Jin, and S,-Y. Hong, 2012: Development of new ensemble methods based on the performance skills of regional climate models over South Korea. *J. Climate*, **25**, 7067-7082.

______, and Coauthors, 2016: Projection of fine-scale climate change using muli-regional climate models and ensembles over South Korea based on four RCP scenarios. Part 1. Surface air temperature. *Asia-Pac. J. Atmos. Sci.*, **52**, doi:10.1007/s13143-016-0017-9.

Sui, Y., X. Lang, and D. Jiang, 2014: Time of emergence of climate signals over China under the RCP4.5 scenario. *Climatic Change*, **125**, 265-276.

Tebaldi, C., and R. Knutti, 2007: The use of the multi model ensemble in probabilistic climate projections. *Phil. Trans. R. Soc. A*, **365**, 2053-2075.

Wilcoxon, F., 1945: Individual comparisons by ranking methods. *Biometrics Bull.*, **1**, 80-83.

Yun, K.-S., K.-Y. Heo, J.-E. Chu, K.-J. Ha, E.-J. Lee, U. Choi, and A. Kitoh, 2012: Changes in climate classification and extreme climate indices from a high-resolution future projection in Korea. *Asia-Pac. J Atmos. Sci.*, **48**, 213-226.

Zhou, L., R. E. Dickinson, P. Dirmeyer, A. Dai, and S.-K. Min, 2009: Spatiotemporal patterns of changes in maximum and minimum temperatures in multi-model simulations. *Geophys. Res. Lett.*, **36**, L02702, doi:10.1029/2008GL036141.